The current issue and full text archive of this journal is available at
www.emeraldinsight.com/1757-9864.htm

Plasticity and damage analysis of metal hollow sphere structures under dynamic compressive loading

Luiz Antônio Bragança da Cunda
Escola de Engenharia,
Universidade Federal do Rio Grande – FURG, Rio Grande, Brazil
Branca Freitas de Oliveira
Virtual Design, Universidade Federal do Rio Grande do Sul,
Porto Alegre, Brazil, and
Guillermo Juan Creus
ILEA, Universidade Federal do Rio Grande do Sul, Porto Alegre, Brazil

Abstract

Purpose – As compared with homogeneous metals and alloys, cellular metals provide low density, high specific stiffness, high energy absorption and good damping, thus being interesting alternatives to employ as protection against shock and impact. Impact energy is dissipated through cell bending, buckling or fracture. The knowledge and computational modelling of the mechanical behaviour of metal foams structures is thus of great importance for real life applications. The purpose of this paper is to increase the knowledge of the differences in metallic hollow sphere structures' (MHSS) behaviour under dynamic loading, as compared with the corresponding behaviour under static loading and to determine the influence of inertia and loading rate.

Design/methodology/approach – Computational dynamical finite element analyses of representative volume elements (RVE) of MHSS have been performed considering varying loading rates. Partially bonded geometries are considered and the effect of the spheres' distribution is also taken into account.

Findings – The results of the numerical examples presented show that inertia plays an important role in the dynamic behaviour of this kind of energy-absorbing structure. When compared with the corresponding values in the quasi-static case, the effect of inertia makes the peak load higher. If the deformation rate is higher (greater than 1.39 m/s in the studied cases), the characteristic plateau usually present in compressed metal foams can vanish. For the geometries analysed, damage has a small influence on load-deformation relations.

Originality/value – This paper presents and discusses differences between static and dynamic behaviour of partially bonded MHSS. There are few references in the literature covering this issue by means of numerical analysis.

Keywords Structures, Dynamic loading, Dynamic analysis, Mechanical behaviour of materials, Metals, Metallic foams, Metallic hollow sphere structures, Plasticity, Damage, Finite elements

Paper type Research paper

The financial support of CNPq (Project 572851/2008-1), CAPES and PROPESQ-UFRGS are gratefully acknowledged.

International Journal of Structural Integrity
Vol. 3 No. 2, 2012
pp. 101-117

1757-9864
DOI 10.1108/17579861211235147

1. Introduction

Cellular metals and metallic foams are materials composed by a metallic matrix with internal voids (Gibson and Ashby, 1997; Ashby *et al.*, 2000). They show mechanical behaviour and physical properties that strongly differ from those of solid materials and offer interesting combinations of properties as, for example, high stiffness combined with low-specific weight, or permeability to gas flow combined with high-thermal conductivity (Haghighi and Kasiri, 2010). Important characteristics of metallic foams are their excellent ability for energy absorption (Nemat-Nasser *et al.*, 2007) and high-specific stiffness (Fiedler, 2007; Öchsner *et al.*, 2003). The combination of such mechanical properties with good sound and heat isolation (Abramenko *et al.*, 1999) opens for these materials a wide field of potential engineering applications.

The schematic stress-strain curve of a metallic foam in compression (Figure 1) shows a large area in the plateau region corresponding to high-energy absorption at constant stress.

The high-strain-rate stress-strain response of metallic foams has received increased attention in recent years because of their potential for energy absorption during deformation under impact. A better understanding of the deformation mechanisms present in these materials would enable designers to more fully utilize their energy absorbing characteristics.

The present authors have published previous reports on the behaviour of cellular metals and MHSS metallic foams (Oliveira *et al.*, 2008, 2009a, b). The aim of the research is to study the static and dynamical behaviour of metal foams by means of computational analyses that takes into account the micro-structure, studying the effects of geometry, loading rate and material properties. The analysis is restricted to compressive loading, which is the dominant input in impact absorption applications. In the present paper, Abaqus is employed to analyze the compressive behaviour of different MHSS geometries under dynamic loading. Using a RVE analysis,

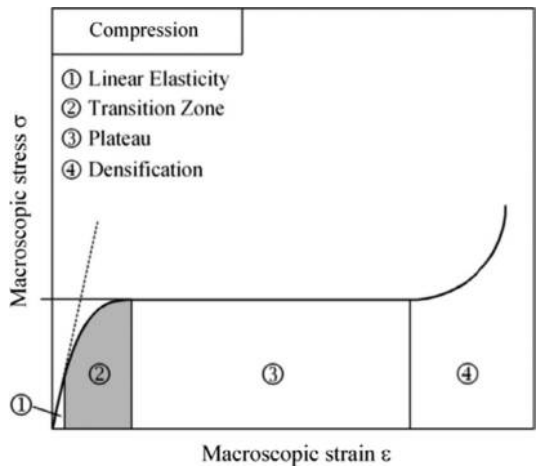

Notes: (1) initial deformation; (2) constant stress plateau and (3) consolidation
Source: Öchsner *et al.* (2003)

Figure 1.
Stress-strain curve for a metallic foam showing large capacity of energy absorption at constant stress

results to the body-centered cubic (BCC) geometry are compared with previous results to the simple cubic (SC) geometry.

In Section 2, a review on some works related with the present study is presented. Section 3 shows the methods and materials used. Section 4 presents and discusses the finite element simulations performed and Section 5 gives the conclusions and final comments. Details of the damage model are given in an Appendix.

2. Review and background

Metal foams can undergo large compressive deformations and absorb considerable amounts of energy. The energy is dissipated through the cell bending, buckling or fracture and stress is fairly constant in the stress-strain curve plateau. Thus, for a given amount of dissipated energy, a foam specimen always shows a maximum force lower than that corresponding to a solid specimen of the base material from which the foam is derived.

On the other hand, the mechanical behaviour of metal foams, particularly under dynamic loading is still not well understood. Important questions to be answered are:

- Dependence of the higher values of stress (peak and plateau values) on impact velocity.
- Dependence of the above stresses on foam topology and base material.
- Analytical bases for approximate or numerical calculations.

The available experimental research shows desirable properties but not well-established quantitative results. For example, in Balch *et al.* (2005), results for syntactic foams fabricated by liquid metal infiltration of commercially pure 7075 aluminium into preforms of hollow ceramic micro-spheres are given. The foams exhibited peak strengths during dynamic loading exceeding in 10-30 per cent the corresponding quasi-static value, with strain rate sensitivities similar to those of aluminium-matrix composite materials. X-ray tomography investigation was used to reveal differences in deformation modes. The foams displayed pronounced energy-absorbing capabilities, suggesting potential in packaging applications and impact protection.

In Cady *et al.* (2009), the compressive constitutive behaviour of a closed-cell aluminium foam (ALPORAS) was evaluated under static and dynamic loading conditions as a function of temperature. A small change in the stress-strain behaviour as a function of strain rate was measured. The deformation behaviour of the Al-foam was found to be strongly temperature dependent under both quasi-static and dynamic loading.

In Montanini (2005), the structural performance of aluminium alloy foams was investigated experimentally under both static and dynamic compressive loads. Three foam typologies (M-Pore, Cymat, Schunk) in a wide range of densities (from 0.14 to 0.75 g/cm^3), made by means of different processes (melt gas injection, powder metallurgy, investment casting) were analyzed to assess their strain rate sensitivity and energy absorption capability and to point out the correlation between the mechanical behaviour and the physical and geometrical properties of the foam. Impact tests showed that the dependence of the plateau stress on the strain rate can be considered negligible for M-Pore and Cymat foams while it is quite remarkable for Schunk foams. Moreover, it was found that the peak stress of Cymat foams has a quite large sensitivity on the loading rate. The review of other experimental reports on dynamic deformation of cellular metals also shows results apparently conflicting

(Paul and Ramamurty, 2000; Mukai *et al.*, 2006; Dannemann and Lankford, 2000; Deshpande and Fleck, 2000; Han *et al.*, 2005; Zhao *et al.*, 2005).

Four causes have been proposed for the rate sensitivity of metallic cellular materials:

(1) the pressure of the air trapped in the cells;

(2) the rate sensitivity of the base materials;

(3) the shock enhancement; and

(4) the micro-inertia effect.

Theoretical calculations by Zhao *et al.* (2005) seem to show that the effect of entrapped air would represent a very small contribution in the case of metallic foams. As for the macroscopic rate sensitivity of the cellular materials, it depends on the rate sensitivity of the base materials. Deshpande and Fleck (2000) found that these two rate sensitivities are of the same order of magnitude. On the other hand, such influence cannot explain all the observed macroscopic rate sensitivity of aluminium foams because the rate sensitivity of aluminium is proved to be very small (Lindholm *et al.*, 1971).

Reid and Peng (1997) reported the strength enhancement by the formation of shock waves which may happen at high-impact speed (about 50 m/s). The basic idea is the possible formation of a unique shock front because the behaviour of cellular materials in their densification part is a concave function. Analytical (Harrigan *et al.*, 2010) and experimental investigations (Zhao *et al.*, 2005) seems to indicate that neither this effect can explain the rate effect on foams.

Thus, the remaining causes are base material rate-dependency (for some materials) and micro-inertia. Micro-inertia effects may include several components, among them those related to dynamic buckling, where the lateral inertia under impact increases strength because inertia increases the resistance to bending. If the load on a column is applied suddenly and then released, the column can sustain a load much higher than its quasi-static (slowly applied) buckling load. This can happen, for example, in a long, unsupported column (rod) used as a drop hammer. The duration of compression at the impact end is the time required for a stress wave to travel up the rod to the other (free) end and back down as a relief wave. Maximum buckling occurs near the impact end at a wavelength much shorter than the length of the rod, at a stress many times the buckling stress if the rod were a statically loaded column (Lindberg, 2003). Lindberg (2003) and Lee *et al.* (2006) study the dynamic elastoplastic buckling of simple models, and show that the relative importance of the strain-rate and inertia effects depends on the impact velocity and the geometry of the structure. Calladine and English (1984), showed that type II structures (Figure 2) (i.e. structures which have a falling quasi-static load-deflection curve, as metal foams after the peak load and before compaction) display more strongly strain-rate and inertia effects under dynamic loading conditions than type I structures (structures with monotonically increasing quasi-static load-deflection curves). Tam and Calladine (1991) conducted further, more detailed experiments on type II structures and pointed out that inertia is the dominant factor in the first phase (their pure compression phase) of the dynamic response to impact, while, in contrast, the second phase, in which energy is dissipated by plastic bending, is more sensitive to strain-rate effects.

In Su *et al.* (1995a, b), a structural model which consists of four compressible elastic-plastic bars connected by four elastic-plastic "hinges" of finite length (Figure 2)

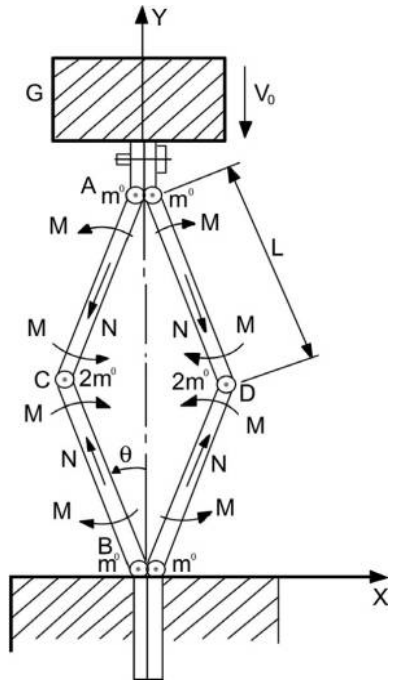

Source: Su *et al.* (1995b)

Figure 2.
A structural model for the analysis of type II structures (structures that show softening behavior after the peak load)

was proposed and its dynamic behaviour under impact loading was analyzed in detail. The analysis shows that inertia appears to be the dominant factor in the entire deformation process and that strain-rate enhances the load-carrying capacity of these types of structures during their entire dynamic deformation.

In another important work (Lee *et al.*, 2006), the quasi-static and dynamic compressive behaviour of pyramidal truss cores made of stainless steel were investigated using a combination of numerical and experimental techniques. Quasi-static tests were performed using a miniature loading frame. A Kolsky bar apparatus was used to investigate intermediate deformation rates and high-deformation rates were examined using a light gas gun. A finite element model was used for simulations intended to understand the roles of material strain rate hardening and structural micro-inertia. Comparison of force-deformation histories under quasi-static and low-deformation rates revealed a moderate micro-inertia effect as manifested by a small increase in peak compressive stress, as shown in Figure 3. At high deformation rates, a major increase in peak compressive stress was observed. In this case, the inertia associated to the bending and buckling of truss struts played a significant role.

Karagiozova and Jones (2000), that studied the dynamic elastic-plastic buckling of cylindrical shells, showed that the buckling phenomenon is governed by the whole complex of loading parameters, boundary conditions and geometrical characteristics of the specimens, so that the interaction between all impact parameters should be considered in any particular case.

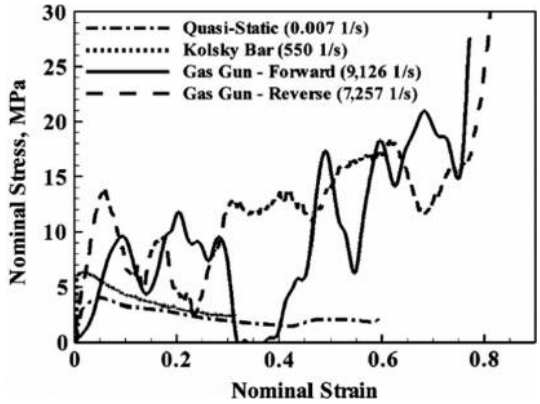

Figure 3.
Stress-strain curves of pyramidal truss core being crushed at different strain rates

Source: Lee *et al.* (2006)

In Oliveira *et al.* (2008), a comparison between representative volume element (RVE) and full mesh approaches for the simulation of compression tests on cellular metals is presented. In Oliveira *et al.* (2009b), MHSS behaviour under quasi-static loading is studied using numerical simulation; the elastoplastic deformation and the damage effects are determined for a single sphere and for groups of spheres and numerical and experimental results are compared. In Oliveira *et al.* (2009a), complementary information on the damage analysis is given. The numerical procedure was used in the crash analysis of a concept car (Cardoso and Oliveira, 2010).

The analysis of a single sphere behaviour showed that damage is localized in a small region at the base of the RVE and has little effect on the load-displacement relation, which depends strongly on boundary conditions (Oliveira *et al.*, 2009b). This dependence is confirmed by the results (Figure 4) with a RVE and a 5×5 cells structure (a square layer with five cells in each direction). The comparison of experimental (Lim *et al.*, 2002) and numerical results showed a fairly good approximation.

In Cunda *et al.* (2011), behaviour of MHSS under dynamic loading is described through the study of cells and cells blocks considering the influence of inertia and strain rate dependency of the base material. The effect of the plastic deformation wave as it travels through the stack of cells is described and shown to coincide with experimental observations in Nemat-Nasser *et al.* (2007). Under lower deformation rates, most of the plastic deformation takes place at the bottom cells (Figure 5), far from the region in which the load is applied, while at higher deformation rates, the cells at the top, in contact with the loading plane, are the most deformed (Figure 6).

3. Materials and methods

The material studied was a MHSS with typical dimensions shown in Figure 7. The metal spheres have an external radius of 1.5 mm and the resin thickness between spheres is 0.36 mm, according the structure of the specimen of MHSS.

Considering a cubic unit cell approach, two geometries were studied, as shown in Figure 8. The first one, a cubic unit cell with a sphere in each corner, associated to a regular stack of spheres bonded by resin in the vertical and horizontal directions, in this work called SC. The second one, a cubic unit cell with a central sphere in addition

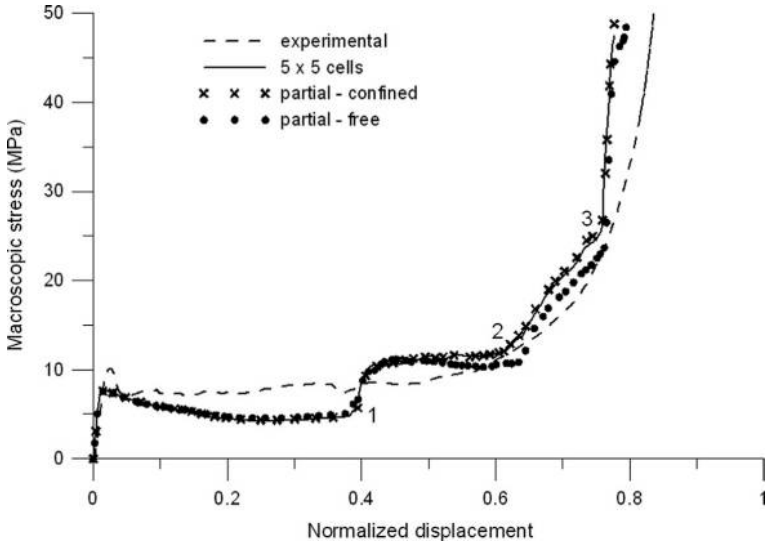

Source: Oliveira *et al.* (2009b)

Figure 4.
Macroscopic stress versus normalized displacement plots considering a confined RVE, a free RVE and the 5×5 cells model

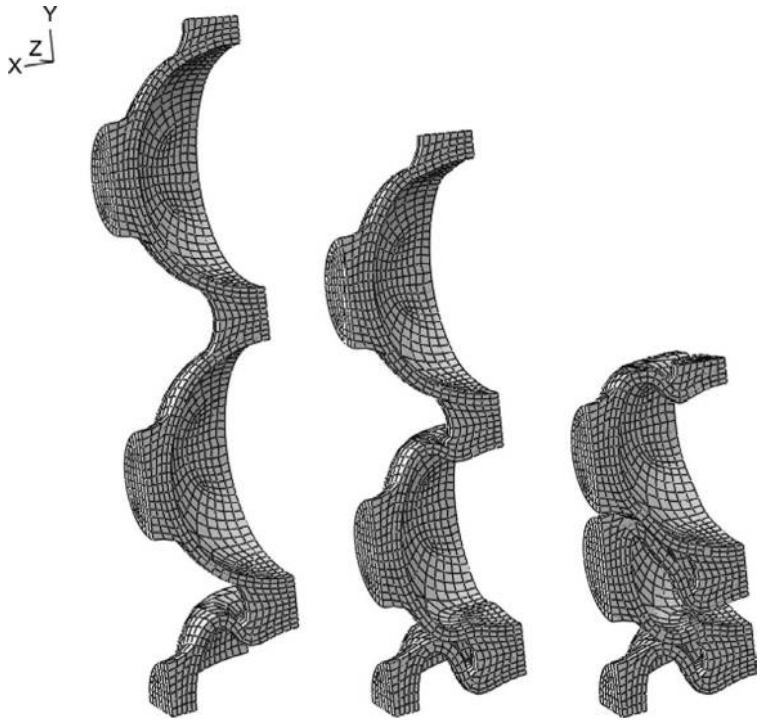

Figure 5.
Deformation of a cells column at 10, 25 and 55 per cent ratios of compression, obtained with an imposed loading velocity of 0.28 m/s

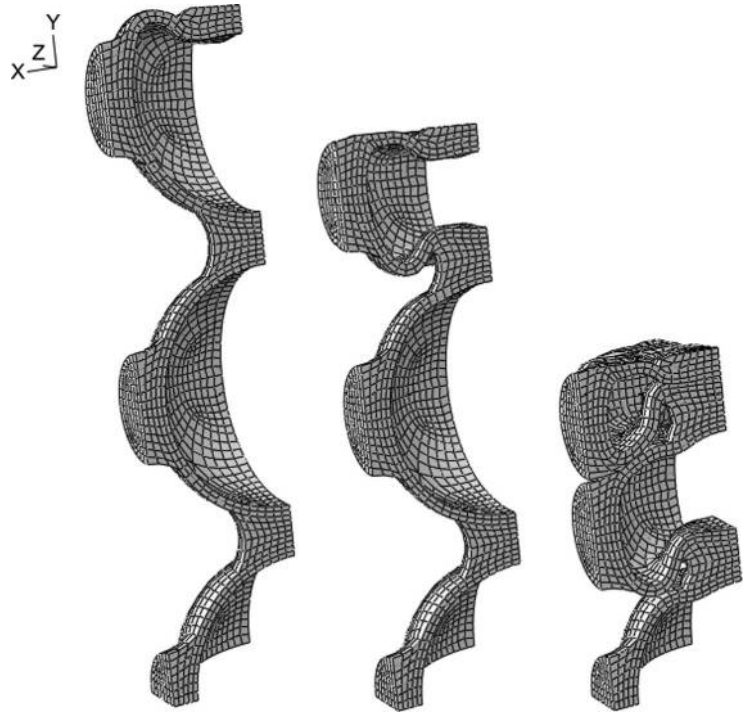

Figure 6.
Deformation of a cells column at 10, 25 and 55 per cent ratios of compression, obtained with an imposed loading velocity of 2.78 m/s

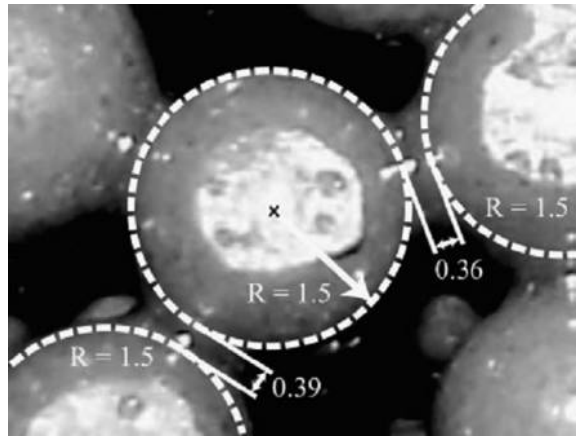

Source: Fiedler (2008)

Figure 7.
MHSS morphology indicating some typical dimensions in millimeter

to the spheres that exists in its corners. This geometry takes into account some level of mortise between layers of spheres, and is called BCC. In this geometry, the central sphere is bonded only to the corner spheres. The corner spheres of each unit cell are not bonded among them.

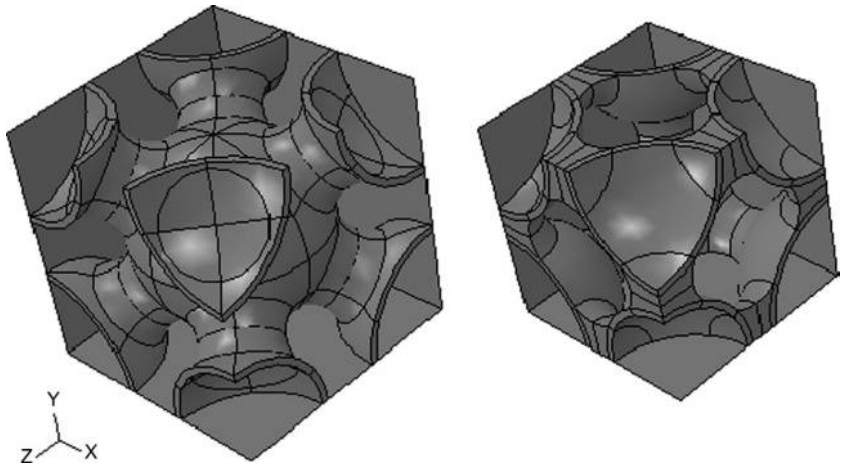

Figure 8.
Body-centered cubic and SC unit cells, respectively

The model used in the numerical simulation was made to fit the MHSS (Figure 7) density of 0.6 g/cm^3 in the case of SC geometry. To define the SC geometry, it was fixed the spheres external diameter of 3 mm, the spheres spacing of 0.36 mm and adjusted the amount of resin. To define the BCC geometry, the distance between central and corner spheres was fixed to 0.36 mm, employing the same volume of resin between spheres, leading to a global density of 0.81 g/cm^3. Considering the adopted hollow spheres diameter and spacing, the edge of SC cell results 3.36 mm length and the edge of BCC cell results 3.88 mm length.

To reduce the size of finite elements mesh, symmetry considerations are employed. The boundary conditions (Figure 9) on the vertical faces reproduce symmetry conditions on the left face and maintaining the right face plane and vertical, but allowing horizontal displacements, in order to represent the average behaviour of the material when a vertical displacement is applied to the top side. Homogeneous deformation boundary conditions lead to a Voigt upper bound while homogeneous stress boundary conditions lead to a Reuss lower bound and periodic boundary conditions lead to an intermediate solution (Li and Wang, 2008). The first alternative was chosen to be on the safe side.

The material parameters were taken as follows. Elastic modulus $E = 110$ GPa, Poisson's ratio $\nu = 0.30$, yield stress $\sigma_y = 300$ MPa and density $\rho = 6.95$ g/cm^3 for the sintered steel of the spheres and $E = 2.46$ GPa, $\nu = 0.36$, yield stress $\sigma_y = 113$ MPa and density $\rho = 1.13$ g/cm^3 for the resin (Fiedler, 2007). Both the metallic spheres and the resin were modelled as elastoplastic without hardening. The metallic spheres were considered as elastoplastic with Gurson damage; the parameters employed were $\alpha_1 = 1.5$, $\alpha_2 = 1.0$, $\alpha_3 = 2.25$, $f_N = 0.04$, $\varepsilon_N = 0.3$ and $s_N = 0.1$. A short review of Gurson formulation (Gurson, 1977; Tvergaard, 1981, 1982; Tvergaard and Needleman, 1984; Koplik and Needleman, 1988) is presented in an Appendix.

4. Finite element simulations

Numerical analyses were performed using Abaqus/Standard and Abaqus/Explicit for static and dynamic simulations, respectively, with automatic time increments size in a geometrically nonlinear context. Abaqus is a sophisticated finite element code

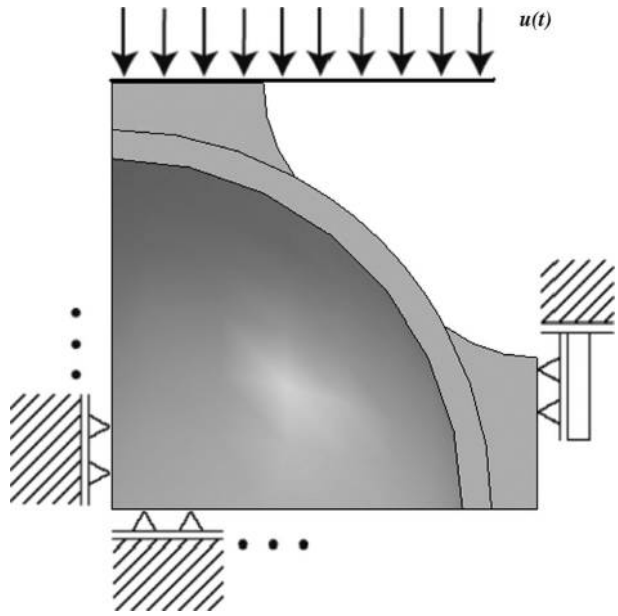

Figure 9.
SC cell – boundary conditions employed

frequently used in high-level research. At the beginning of our work with metallic foams we used both an in-house program and Abaqus. As the corresponding results were very close, we are working now with Abaqus, that being an easily available code, it may allow the verification and eventual extension of our results.

In both static and dynamic simulations 3D, eight node linear isoparametric elements with full reduced integration were used (C3D8R). The mesh was determined through previous convergence tests. Figures 10 and 11 show the meshes employed to study the SC and BCC geometries, respectively. Sliding contact was assumed.

Obtained results are shown as macroscopic stress (defined as the ratio between the sum of the reaction forces in the loading direction and the square surface corresponding to the projection of the undeformed cubic cell onto a plane) versus normalized displacement (defined as the relation between the imposed displacement to the top plane and the original cell height).

Looking to the results obtained in the numerical analysis of single cells (Figure 12), it can be seen that the plateaulevel is higher to the BCC geometry as compared to that observed to the SC geometry. Similar behaviour happens with the slope of the initial elastic zone, in which BCC cell exhibits higher values than those to the SC cell.

Comparing the single cell numerical results with experimental results, it is clear that the SC geometry fits better the experimental results, especially in the plateau region. It must be remarked that the dimensions of the resin region were defined to fit the experimental density in the SC geometry, while in the BCC geometry was maintained the same volume of resin in the union of neighbour spheres. Due to the nature of the geometries, the density results greater in the BCC geometry than in the SC one.

Another aspect to be considered are the localized stiffness changes that SC model exhibits (points 1, 2 and 3 of Figure 4) especially at 0.4 normalized displacement.

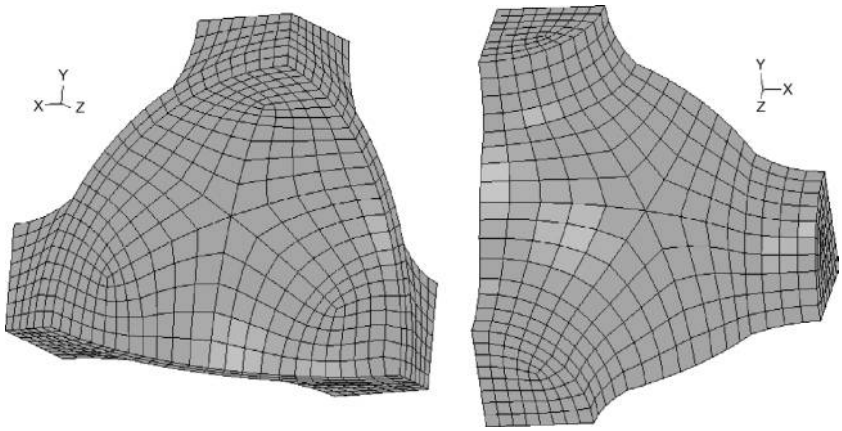

Figure 10.
SC cell – finite element mesh employed

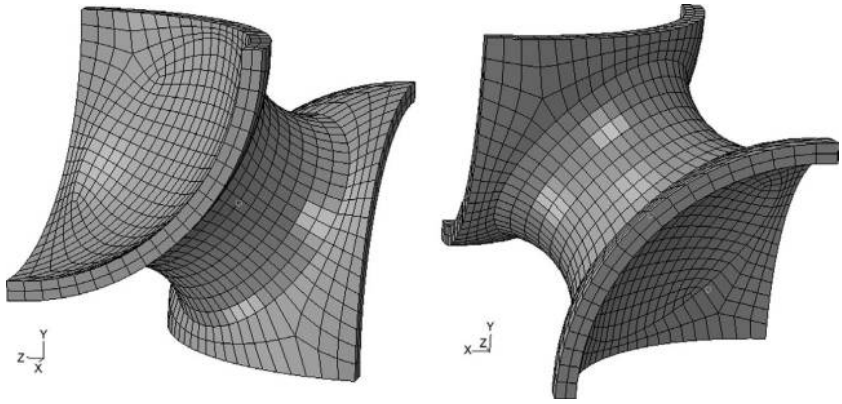

Figure 11.
Body-centered cubic cell – finite element mesh employed

The experimental results do not show this behaviour because in a real foam, the geometric distribution of the spheres is not so regular as in the model employed, so the contact between neighbour spheres takes place incrementally (Oliveira *et al.*, 2009b), not showing an abrupt change in stiffness. In this aspect, BCC geometry presents a smoother plateau than the SC geometry, due to the nature of its topology.

The deformation of SC cell is shown in Figure 13 and the deformation of BCC cell is shown in Figure 14.

Figure 15 shows the final distribution of volumetric void fraction (VVF) to the SC cell. It can be seen that the damage is localized in a small region where the sphere is not confined by the resin. The final values reached are low as well as their influence on the load-deformation plot.

Considering the dynamical analysis of a SC single cell, it can be observed that dynamic loading modifies the value and the localization of the peak load. The higher the velocity the higher are the peak stress and the normalized displacement value for its occurrence, as shown in Figure 16.

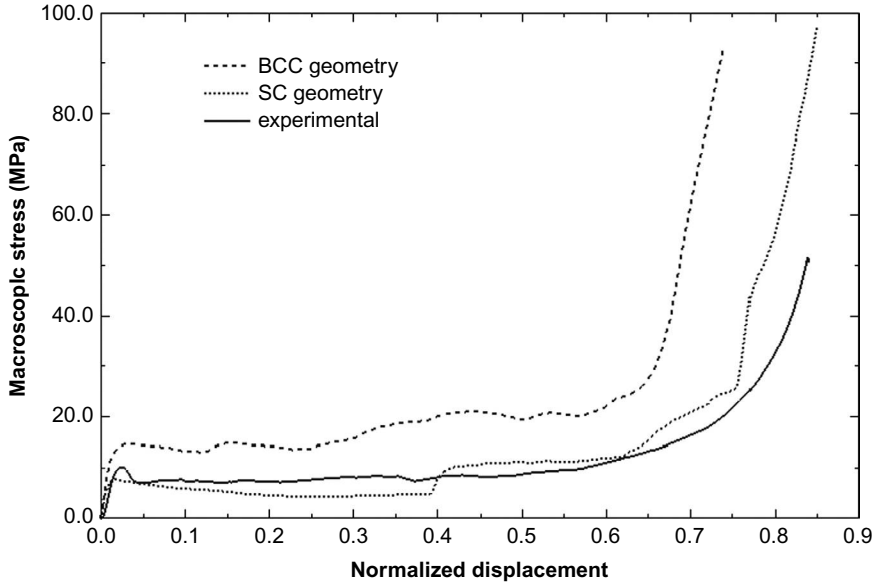

Figure 12.
Experimental and numerical results of macroscopic stresses, considering the SC and BCC geometries

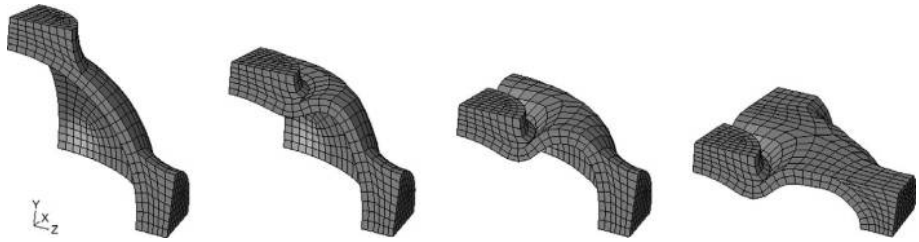

Figure 13.
SC geometry at 0, 25, 50 and 75 per cent ratios of compression, respectively

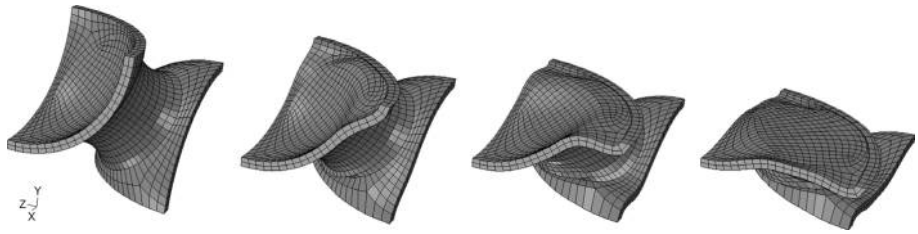

Figure 14.
BCC geometry at 0, 25, 50 and 74 per cent ratios of compression, respectively

Looking to the Figure 17, it can be seen that if deformation rate grows, the plateau stress level grows together. For higher deformation rates the plateau region is altered. In the dynamical results an initial peak of stress between the initial elastic zone and the plateau can be identified. This stress peak is undesirable if the material is to be used as a protection against impacts. Similar behaviour can be found in SC and BCC cells, but in a more intense way in the SC cells.

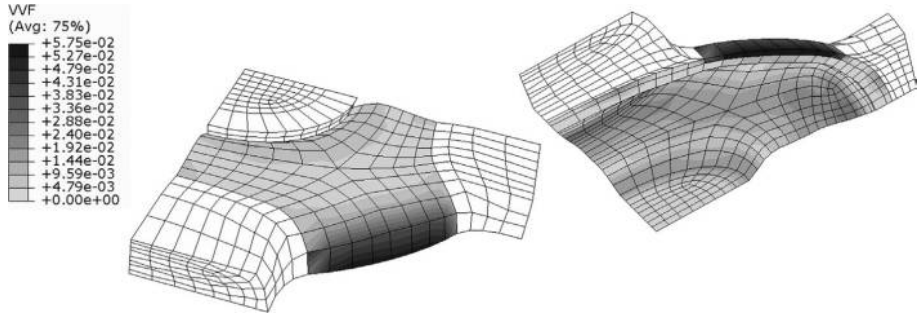

Figure 15.
Final VVF distribution for the SC geometry

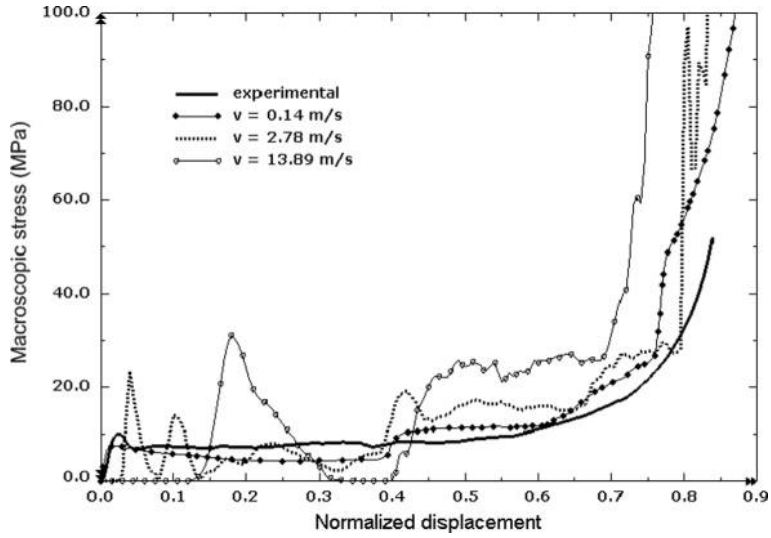

Figure 16.
Macroscopic stress plots showing experimental and numerical results for the quasi-static case and numerical results for the dynamical analyses with SC geometry

5. Conclusions and final remarks

The main contribution of the present paper is the extension of a computational procedure that uses micro-mechanical techniques (Oliveira *et al.*, 2008, 2009a, b) to study the effect of inertia forces on the deformation behaviour of MHSS metal foams. Here, the load-deformation behaviour of the SC and BCC geometries under compressive dynamical loading was determined. Both the importance of foam geometry and impact velocity were analysed.

The increase of the initial peak load with impact speed is determined. For the higher speeds (>1.39 m/s in the studied cases), the characteristic shape of the plateau is modified, as a comparison of Figure 12 (quasi-static analysis) and Figures 16 and 17 (dynamical analysis) shows. Experimental results (Figure 3) corroborate this behaviour. These effects are more evident in the SC geometry than in the BCC geometry. Thus, the capacity to absorb energy at a constant stress observed in the quasi-static case is partially lost in a dynamic situation. This effect is important and has to be taken into account in industrial applications.

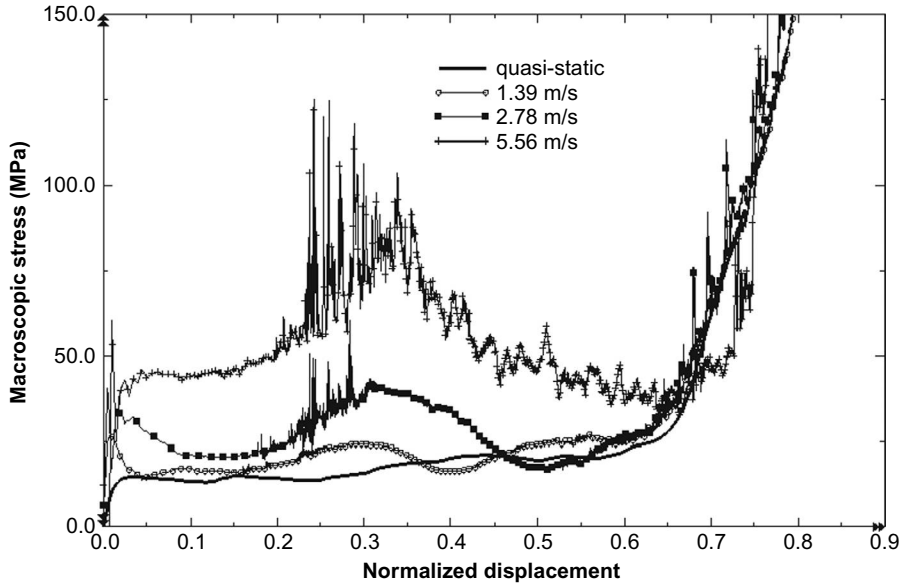

Figure 17.
Macroscopic stress plots showing numerical results for the quasi-static and dynamical analyses with BCC geometry

The results above are consistent with the experimental findings as reviewed in Section 2. Also, the analysis of a column of spheres shows the advance of the strain wave, reproduces the behaviour observed in experiments (Nemat-Nasser *et al.*, 2007).

Damage reaches low values ($f < 6$ per cent) and is localized in small regions (Figure 15), so it has a very small influence on the load-deformation plots.

The present numerical analysis was restricted to the compressive case, which is the most important in energy-absorption applications. However, the same procedure may be extended, using Abaqus and the information in the Appendix, to other stress states.

References

Abramenko, A.N., Kalinichenko, A.S., Burtser, Y., Kalinichenko, V.A., Tanaeva, S.A. and Vasilenko, I.P. (1999), "Determination of the thermal conductivity of foam aluminium", *Journal of Engineering Physics and Thermophysics*, Vol. 72 No. 3, pp. 369-73.

Ashby, M.F., Evans, A., Fleck, N.A., Gibson, L.J., Hutchinson, J.W. and Wadley, H.N.G. (2000), *Metal Foams: A Design Guide*, Butterworth-Heinemann, Oxford.

Balch, D.K., O'Dwyer, J.G., Davis, G.R., Cady, C.M., Gray, G.T. III and Dunan, D.C. (2005), "Plasticity and damage in aluminum syntactic foams deformed under dynamic and quasi-static conditions", *Materials Science & Engineering A*, Vol. 391, pp. 408-17.

Cady, C.M., Gray, G.T. III, Liu, C., Lovato, M.L. and Mukai, T. (2009), "Compressive properties of a closed-cell aluminum form as a function of strain rate and temperature", *Materials Science & Engineering A*, Vol. 525, pp. 1-6.

Calladine, C.R. and English, R.W. (1984), "Strain-rate and inertia effects in the collapse of two types of energy-absorbing structure", *International Journal of Mechanical Sciences*, Vol. 26, pp. 689-701.

Cardoso, E. and Oliveira, B.F. (2010), "Study of the use of metallic foam in a vehicle for an energy-economy racing circuit", *Materialwissenschaft und Werkstofftechnik*, Vol. 41, pp. 257-64.

Cunda, L.A.B., Oliveira, B.F. and Creus, G.J. (2011), "Plasticity and damage analysis of metal foams under dynamic loading", *Mecánica Computacional*, Vol. 42, pp. 356-64.

Dannemann, K.A. and Lankford, J. (2000), "High strain rate compression of closed-cell aluminium foams", *Material Science and Engineering A*, Vol. 293, pp. 157-64.

Deshpande, V.S. and Fleck, N.A. (2000), "High strain-rate compressive behaviour of aluminium alloy foams", *International Journal of Impact Engineering*, Vol. 24, pp. 277-98.

Fiedler, T. (2007), "Numerical and experimental investigation of hollow sphere structures in sandwich panels", PhD thesis, University of Aveiro, Aveiro.

Fiedler, T. (2008), "Numerical and experimental investigation of hollow sphere structures in sandwich panels", Materials Science Foundations, v. 44, Trans Tech Publications, Zurich.

Gibson, L.J. and Ashby, M.F. (1997), *Cellular Solids, Structure and Properties*, 2nd ed., Cambridge University Press, Cambridge.

Gurson, A.L. (1977), "Continuum theory of ductile rupture by void nucleation and growth: part I. Yield criteria and flow rules for porous ductile media", *ASME Journal of Engineering Materials and Technology*, Vol. 99, pp. 2-15.

Haghighi, M. and Kasiri, N. (2010), "Estimation of effective thermal conductivity enhancement using foam in heat exchangers based on a new analytical model", *Brazilian Journal of Chemical Engineering*, Vol. 27, pp. 127-35.

Han, F.S., Cheng, H.F., Li, Z.B. and Wang, Q. (2005), "The strain rate effect of an open cell aluminum foam", *Metallurgical and Materials Transactions A*, Vol. 36, pp. 645-50.

Harrigan, J.J., Reid, S.R. and Seyed Yaghoubi, A. (2010), "The correct analysis of shocks in a cellular material", *International Journal of Impact Engineering*, Vol. 37, pp. 918-27.

Karagiozova, D. and Jones, N. (2000), "Dynamic elastic-plastic buckling of cylindrical shells under axial impact", *International Journal of Solids and Structures*, Vol. 37, pp. 2005-34.

Koplik, J. and Needleman, A. (1988), "Void growth and coalescence in porous plastic solids", *International Journal of Solids and Structures*, Vol. 24, pp. 835-53.

Lee, S., Barthelat, F., Hutchinson, J.W. and Espinosa, H.D. (2006), "Dynamic failure of metallic pyramidal truss core materials – experiments and modelling", *International Journal of Plasticity*, Vol. 22, pp. 2118-45.

Li, S. and Wang, G. (2008), *Introduction to Micromechanics and Nanomechanics*, World Scientific, Singapore.

Lim, T.J., Smith, B. and McDowell, D.L. (2002), "Behavior of a random hollow sphere metal foam", *Acta Materialia*, Vol. 50, pp. 2867-79.

Lindberg, H.E. (2003), *Little Book of Dynamic Buckling*, LCE Science/Software, Penn Valley CA.

Lindholm, U.S., Bessey, R.L. and Smith, G.V. (1971), "Effect of strain rate on yield strength and elongation of three aluminum alloys", *Journal of Materials*, Vol. 6, pp. 119-33.

Montanini, R. (2005), "Measurement of strain rate sensitivity of aluminium foams for energy dissipation", *International Journal of Mechanical Sciences*, Vol. 47, pp. 26-42.

Mukai, T., Miyoshi, T., Nakano, S., Somekawa, H. and Higashi, K. (2006), "Compressive response of a closed-cell aluminum foam at high strain rates", *Scripta Materialia*, Vol. 54, pp. 533-7.

Nemat-Nasser, S., Kang, W.J., McGee, J.D., Guo, W.G. and Isaacs, J. (2007), "Experimental investigation of energy-absorption characteristics of components of sandwich structures", *International Journal of Impact Engineering*, Vol. 34, pp. 1119-46.

Öchsner, A., Winter, W. and Kuhn, G. (2003), "On an elastic-plastic transition zone in cellular metals", *Archives of Applied Mechanics*, Vol. 73, pp. 261-9.

Oliveira, B.F., Cunda, L.A.B. and Creus, G.J. (2009a), "Modeling of the mechanical behavior of metallic foams: damage effects at finite strains", *Mechanics of Advanced Materials and Structures*, Vol. 16, pp. 110-19.

Oliveira, B.F., Cunda, L.A.B., Öchsner, A. and Creus, G.J. (2008), "Comparison between RVE and full mesh approaches for the simulation of compression tests on cellular metals", *Materialwissenschaft und Werkstofftechnik*, Vol. 39, pp. 133-8.

Oliveira, B.F., Cunda, L.A.B., Öchsner, A. and Creus, G.J. (2009b), "Hollow sphere structures: a study of mechanical behaviour using numerical simulation", *Materialwissenschaft und Werkstofftechnik*, Vol. 40, pp. 144-53.

Paul, A. and Ramamurty, U. (2000), "Strain rate sensitivity of a closed-cell aluminium foam", *Materials Science & Engineering A*, Vol. 281, pp. 1-7.

Reid, S.R. and Peng, C. (1997), "Dynamic uniaxial crushing of wood", *International Journal of Impact Engineering*, Vol. 19, pp. 531-70.

Su, X.Y., Yu, T.X. and Reid, S.R. (1995a), "Inertia-sensitive impact energy-absorbing structures, Part I: effects of inertia and elasticity", *International Journal of Impact Engineering*, Vol. 16, pp. 651-72.

Su, X.Y., Yu, T.X. and Reid, S.R. (1995b), "Inertia-sensitive impact energy-absorbing structures, Part II: effects of strain rate", *International Journal of Impact Engineering*, Vol. 16, pp. 673-89.

Tam, L.L. and Calladine, C.R. (1991), "Inertia and strain-rate effects in a simple plate-structure under impact loading", *International Journal of Impact Engineering*, Vol. 11, pp. 349-77.

Tvergaard, V. (1981), "Influence of voids on shear band instabilities under plane strain conditions", *International Journal of Fracture*, Vol. 17, pp. 389-407.

Tvergaard, V. (1982), "On localization in ductile materials containing spherical voids", *International Journal of Fracture*, Vol. 18, pp. 237-52.

Tvergaard, V. and Needleman, A. (1984), "Analysis of the cup-cone fracture in a round tensile bar", *Acta Metallurgica*, Vol. 32, pp. 157-69.

Zhao, H., Elnasri, I. and Abdennadher, S. (2005), "An experimental study on the behaviour under impact loading of metallic cellular materials", *International Journal of Mechanical Sciences*, Vol. 47, pp. 757-74.

Appendix. Gurson plasticity-damage model

The Gurson damage model (Gurson, 1977; Tvergaard, 1982) was developed to describe the mechanical effect of high-plastic deformations in ductile metals. The loss of resistance is governed by the porosity level. The (isotropic) damage variable employed is the VVF, represented by f and defined by $f = V_v/V$, where V_v is the volume of voids in a representative small volume V, corrected for effects such as stress concentration; f is defined at each point of the continuum. The presence of voids alters the elastoplastic constitutive relations leading to a yield surface defined by:

$$\Phi = \sqrt{\frac{3}{2}\, s_{ij} s_{ij}} - \bar{\omega}\sigma_y = 0, \tag{A1}$$

where:

$$\bar{\omega} = \left[1 - 2\alpha_1 f \cosh\left(-\frac{\alpha_2 3p}{2\sigma_y}\right) + \alpha_3 f^2\right]^{1/2} \tag{A2}$$

and $s_{ij} = \sigma_{ij} + p\delta_{ij}, \quad p = -1/3\sigma_{ij}\delta_{ij}$.

In the equations above σ_{ij} are the Cauchy stresses and σ_y is the yield stress in simple tension. The adopted values to the yield surface material parameters in Equation (A-2) are $\alpha_1 = 1.5$, $\alpha_2 = 1.0$ and $\alpha_3 = (\alpha_1)^2$. The plastic strain rate tensor is given by $D_{ij}^p = \dot{\lambda}\partial\Phi/\partial\sigma_{ij}$, where $\dot{\lambda}$

is a plastic multiplier. The equivalent plastic strain rate is defined by $\dot{\varepsilon}^p = \sqrt{2/3 D^p_{ij} D^p_{ij}}$. When $\bar{\omega} = 0$, Equation (A-1) reduces to von Mises plasticity without hardening.

The mechanisms of damage evolution are nucleation, growth and coalescence of voids. The equations that govern damage evolution are modelled in a simplified form as follows. First, it is assumed that total void rate is given by:

$$\dot{f} = \begin{cases} \dot{f}_n + \dot{f}_g & f \leq f_C \\ \dot{f}_c & f > f_C \end{cases}, \tag{A3}$$

where f_C is the coalescence onset and $\dot{f}_n, \dot{f}_g, \dot{f}_c$ are the nucleation, growth and coalescence rates.

The nucleation rate is proportional to the equivalent plastic strain rate $\dot{f}_n = A(\varepsilon^p)\dot{\varepsilon}^p$, where

$$A(\varepsilon^p) = \frac{f_N}{s_N \sqrt{2\pi}} \exp\left[-\frac{1}{2} \left(\frac{\varepsilon^p - \varepsilon_N}{s_N} \right)^2 \right] \tag{A4}$$

f_N is the nucleation void volumetric fraction, ε_N is the plastic strain value for nucleation and s_N is the standard deviation for the distribution. Nucleation takes place only with negative pressure (i.e. tension).

Voids increase or decrease their volume according to the volume variation in the continuum. The growth rate of voids is controlled by mass conservation through the expression $\dot{f}_g = (1 - f) D^p_{ii}$.

The coalescence rate can be modeled (Tvergaard and Needleman, 1984) replacing the VVF f in the Gurson yield surface (equation A-1) by a corrected VVF f^*, given by:

$$f^* = \begin{cases} f & f \leq f_C \\ f_C + \frac{1 - f_C}{f_F - f_C}(f - f_C) & f > f_C \end{cases}, \tag{A5}$$

where f_F is a material parameter. In this case, only nucleation and growth are considered in equation A-3.

About the authors

Luiz Antônio Bragança da Cunda is Professor at the Engineering School, FURG. His research interests include: mechanical behaviour of materials and structures, finite elements method, plasticity, large strains and continuum damage mechanics. Luiz Antônio Bragança da Cunda is the corresponding author and can be contacted at: luizcunda@furg.br

Branca Freitas de Oliveira is Professor at UFRGS and Researcher of Productivity at CNPq. She has experience in civil and mechanical engineering, focusing on mechanics of solids, acting on the following subjects: new materials, composite materials, finite elements, constitutive models, failure, ageing, damage, viscoelasticity and plasticity.

Guillermo Juan Creus is Professor at the Engineering School, UFRGS and Director of ILEA. His research interests include: mechanical behavior of materials and structures, viscoelasticity, plasticity and mechanical analysis.